UDC: 549.641.1; 661.8; 621.315.61; 621.317 doi: 10.33609/2708-129X.86.11.2020.13-23

SYNTHESIS AND DIELECTRIC PROPERTIES OF $La_{0.67}Li_xTi_{1-x}Al_xO_3$ (0.15≤x≤0.3) CERAMICS

T. O. Plutenko, O. I. V'yunov *, B. S. Khomenko, A. G. Belous

V. I. Vernadsky Institute of *General and Inorganic Chemistry, Akademik Palladin Avenue 32/34, Kyiv 03142 Ukraine*
E-mail: vyunov@ionc.kiev.ua

ABSTRACT. Solid solutions of Al-doped lithium lanthanum titanates $La_{0.67}Li_xTi_{1-x}Al_xO_3$ system (where $0.15 \le x \le 0.3$) have been synthesized by solid-state reaction technique. Light optical microscopy has shown that the grain size of $La_{0.67}Li_xTi_{1-x}Al_xO_3$ ceramics insignificantly increases with an increase in lithium/aluminum concentration. The materials $La_{0.67}Li_xTi_{1-x}Al_xO_3$ show very high dielectric permittivity $\varepsilon' > 10^4$ over a relatively wide frequency range ($10^2 \le f \le 10^4$ Hz) with no apparent dependence on the x. The impedance spectroscopy study indicates three semicircles on Cole-Cole diagram that can be attributed to electrically different areas of ceramic's grain.

Key words: solid solution, lithium-lanthanum titanate-aluminate, complex impedance, dielectric properties.

INTRODUCTION. Materials with perovskite-related structure (ABO_3) are interesting candidates for a great variety of applications [1, 2]. The compounds of general formula $La_{2/3-x}Li_{3x}TiO_3$ the material substrate for making good ionic conductors [3, 4] and, in particular, lithium has been shown to move in some perovskite systems faster than in any other materials [5, 6]. A large amount of research has been focused on the Ti cation substitution in the $La_{2/3-x}Li_{3x}TiO_3$ system (in particular, at x=1/6, $La_{0.5}Li_{0.5}TiO_3$) by other metal ions with less tendency toward reduction against Li metal. Simultaneous lithium addition and titanium substitution by aluminum in the system $La_{2/3}Li_xTi_{1-x}Al_xO_3$ has been investigated in work [7–10]. Crystal structure of high temperature $La_{2/3}Li_xTi_{1-x}Al_xO_3$ phase with $0.06 \le x \le 0.2$ annealed and quenched from 1273 K was determined [11–13]. Depending on the cooling conditions, the structure can be a perovskite-related orthorhombic or rhombohedral. In the case of an orthorhombic structure, the formation of a superstructure of the basic perovskite is due to two mechanisms: the tilting of octahedra $(Ti/Al)O_6$ and the ordering of La^{3+} and Li^+. The lithium ions are not located at the interstitial A positions of the perovskite structure and their coordination polyhedra is a square pyramid with lithium ion at the apex. Therefore, there is a large amount of non-occupied interstitial positions of this kind for the

lithium ions to move to, and this is likely to be the reason for the very high ionic conductivity of these kinds of materials (~ $8 \cdot 10^5$ S/cm for the oxide with x = 0.25) [12]. In the case of a rhombohedral structure [11, 14] twisting of TiO_6 octahedra is observed in the structure in order to optimize the distances between oxygen and lanthanum ions. Lithium ions are bonded to four oxygen atoms in a square configuration. This environment for Li is different from the tetrahedral-like coordination.

Another interesting property of the $La_{2/3}Li_{x}Ti_{1-x}Al_xO_3$ oxides is their dielectric behavior. The authors recently reported a "giant" barrier layer capacitance effect in $La_{0.67}Li_{0.25}Ti_{0.75}Al_{0.25}O_3$ [9]. It has been demonstrated that the origin of the high dielectric constant ($\varepsilon = 2 \cdot 10^5$, tg δ=0.5 for $La_{0.67}Li_{0.2}Ti_{0.8}Al_{0.2}O_3$ and $\varepsilon = 5 \cdot 10^5$, tg δ=0.5 for $La_{0.67}Li_{0.25}Ti_{0.75}Al_{0.25}O_3$ at $10 \le f \le 10^3$ Hz) can be attributed to a barrier layer capacitor associated with grain boundary effects in the ion-conducting material [8].

However, dielectric behavior was investigated only for an orthorhombic structure sintered with subsequent quenching. While for the practically important case, when the material is obtained by slow cooling and has a rhombohedral structure, dielectric behavior remains unexplored.

Therefore, in this work for the first time dielectric properties of partially substituted complex low-temperature phase $La_{0.67}Li_xTi_{1-x}Al_xO_3$ (where $0.15 \le x \le 0.3$) solid solutions with rhombohedral crystal structure have been investigated. For this, impedance spectroscopy data, recorded at room temperature, have been analyzed. Light optical microscopy has been finally used to analyze the influence of lithium/aluminum concentration on the microstructure of these perovskites. For comparison, $La_{0.5}Li_{0.5}TiO_3$ sample, which has a larger number of lithium ions in the structure was investigated.

EXPERIMENTAL SECTION. Samples were obtained from stoichiometric amounts of dried Li_2CO_3 (Merck), Al_2O_3 (Merck), La_2O_3 (Aldrich 99.99%), and TiO_2 (Aldrich 99 %) by solid-state reaction technique. Li_2CO_3 was dried at 300 °C, La_2O_3 at 800 °C and Al_2O_3, TiO_2 at 600 °C. The mixtures were ground in an agate mortar with acetone, and calcined in air for 6 h at 1200 °C. The rate of temperature increase was 200 °C/hour. The phases were characterized by X-ray powder diffractometry (XRPD) using DRON-4-07 diffractometer (Cu *K*α radiation, λ = 1.54178 Å; 40 kV, 20 mA). The unit cell parameters of the samples were determined using FullProf software by the whole-pattern profile-matching Le Bail procedure [15]. The calcined powders were ground and pressed into pellets with a diameter of 8 mm and a thickness of 2 mm under a pressure of 500 kg/cm^2 (50MPa). The pellets were sintered at 1270–1300 °C depending on Li/Al content (6 h) and were cooled to air temperature with a cooling rate 200 °C/h. Finally, samples with 1 mm thickness were cut out from prepared raw ceramic.

Grain sizes of ceramic samples of $La_{0.67}Li_{x}Ti_{1-x}Al_xO_3$ ($0.15 \le x \le 0.3$) system were determined using an optical microscope LOMO MBS-10. Using a semi-automatic computer program imageJ [16] the area of the grain was measured, mathematically found the nominal diameter, equating the resulting area to the area of the circle. The average value of the measured nominal grain diameters was considered the nominal diameter of the characteristic grain. At least 50 grains were measured from three different areas [17]. Sintered cylindrical pellets 8 mm in

diameter and 2 mm thick, with evaporated metal electrodes, were used for electrical measurements. Impedance spectroscopy measurements were conducted using a 1260 Impedance / Gain phase Analyzer (Solartron Analytical).

RESULTS AND DISCUSSION. It has been shown that single-phase solid solutions $La_{0.67}Li_xTi_{1-x}Al_xO_3$ (where $0.15 \le x \le 0.3$) are formed at temperatures above 1200 °C using solid-state reaction technique.

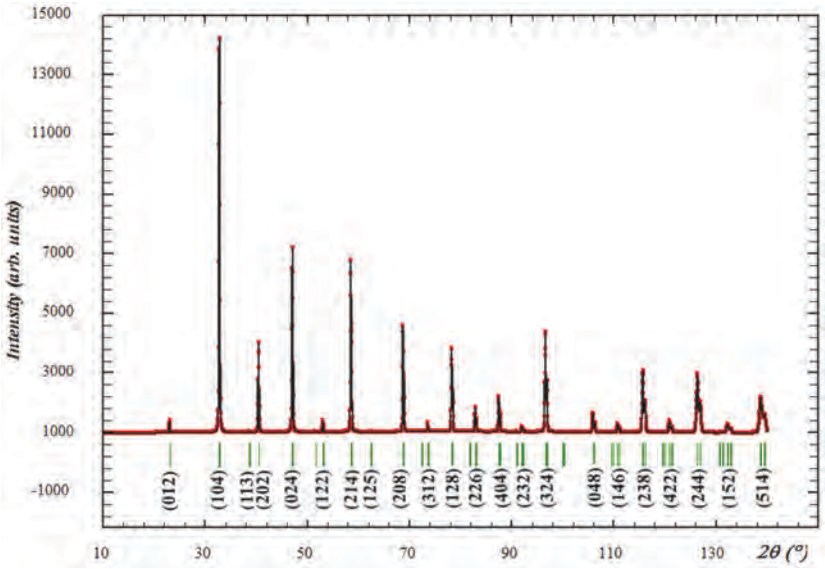

Fig. 1. Experimental (dots) and calculated (line) room-temperature powder X-ray powder diffraction patterns of ceramic samples $La_{0.67}Li_{0.3}Al_{0.3}Ti_{0.7}TiO_3$ sintered at 1300 °C for 2 h. Bars indicate the peak positions.

The unit cell parameters were determined from the XRPD patterns using a rapid whole-pattern profile-matching Le Bail procedure (**Fig. 1**). $La_{0.67}Li_xTi_{1-x}Al_xO_3$ solid solutions (where $0.15 \le x \le 0.3$) materials have a rhombohedral perovskite-related structure (space group $R\bar{3}c$, № 167). In XRPD spectra additional lines of small amount $La_{0.67}Li_xTi_{1-x}Al_xO_3$ with tetragonal phase symmetry (space group P4/mmm, № 123) are observed. The phases observed do not differ in chemical composition. The main difference between these phases is in the crystal structure. Unit cell parameters depend on Li/Al concentration (**Fig. 2**).

Fig. 2 shows the dependence of the unit cell volume of the samples $La_{0.67}Li_xTi_{1-x}Al_xO_3$ system sintered at 1300 °C for 2 h. For the sample x = 0 the data given in [18] was used. The dependence is linear and obeys Vegard's law, which indicates the formation of a continuous series of solid solutions in $La_{0.67}Li_xTi_{1-x}Al_xO_3$ ($0.15 \le x \le 0.3$). Unit cell volume decreases with an increase in x, due to the difference in ionic radii of aluminum and titanium.

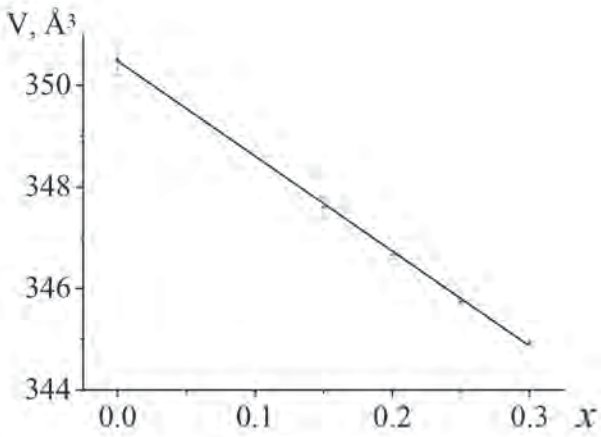

Fig. 2. Unit cell volume of $La_{0.67}Li_xTi_{1-x}Al_xO_3$ solid solutions sintered at 1300 °C for 2 h.

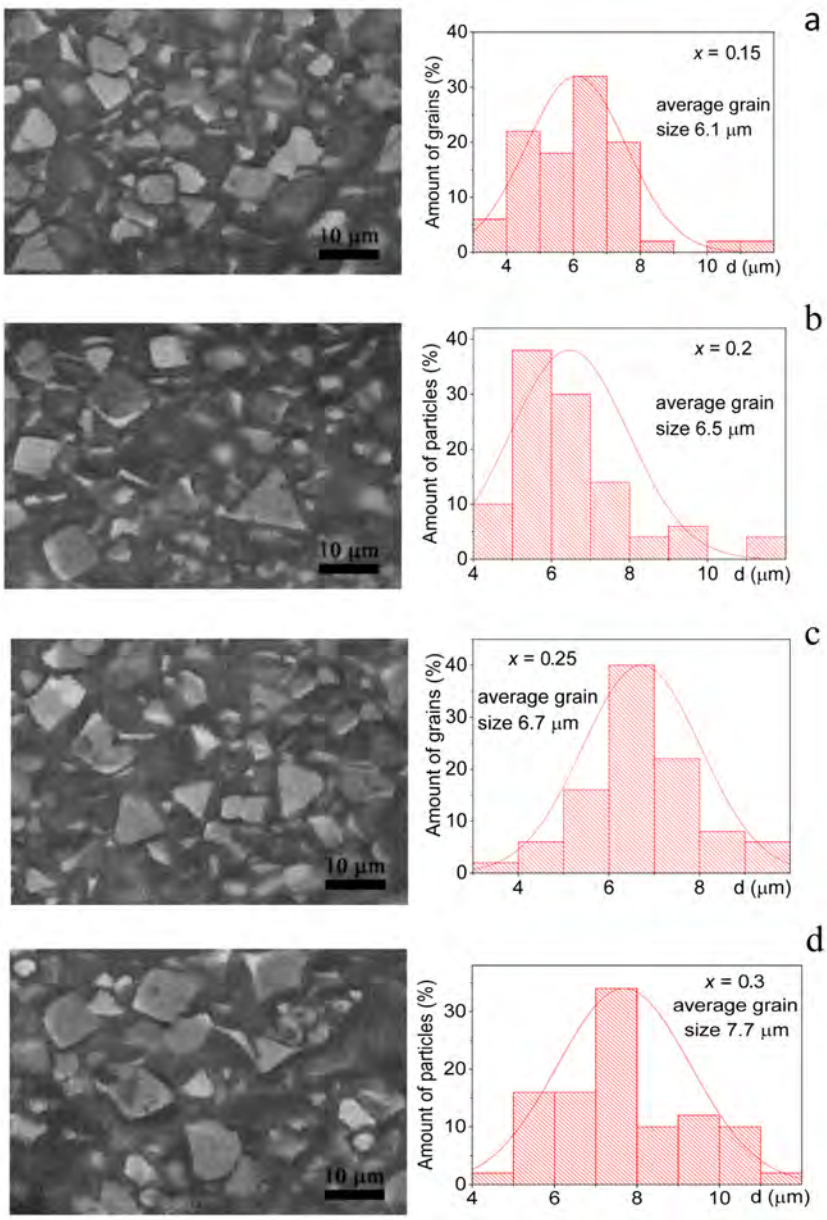

Fig. 3. Optical microscope images of $La_{0.67}Li_xTi_{1-x}Al_xO_3$ ceramics, where x=0.15 (a), 0.2 (b), 0.25 (c), 0.3 (d).

The ceramic's size and morphology of $La_{0.67}Li_xTi_{1-x}Al_xO_3$ were studied by light optical microscopy (**Fig. 3**). It has been shown in **Fig. 3** that with an increase in x, the average grain size slightly increases from 6.1 μm (x=0.15) to 7.7 μm (x=0.3). This fact can be attributed to an increase in sintering temperature with an increase in Li/Al content. The boundary between one grain and another is a defect in the crystal structure and so it is associated with a certain amount of energy [19]. As a result, there is a thermodynamic driving force for the total area of boundary to be reduced. With sintering temperature growth in $La_{0.67}Li_xTi_{1-x}Al_xO_3$ grain size

increases accompanied by a reduction in the number of grains, therefore the total area of the grain boundary is reduced.

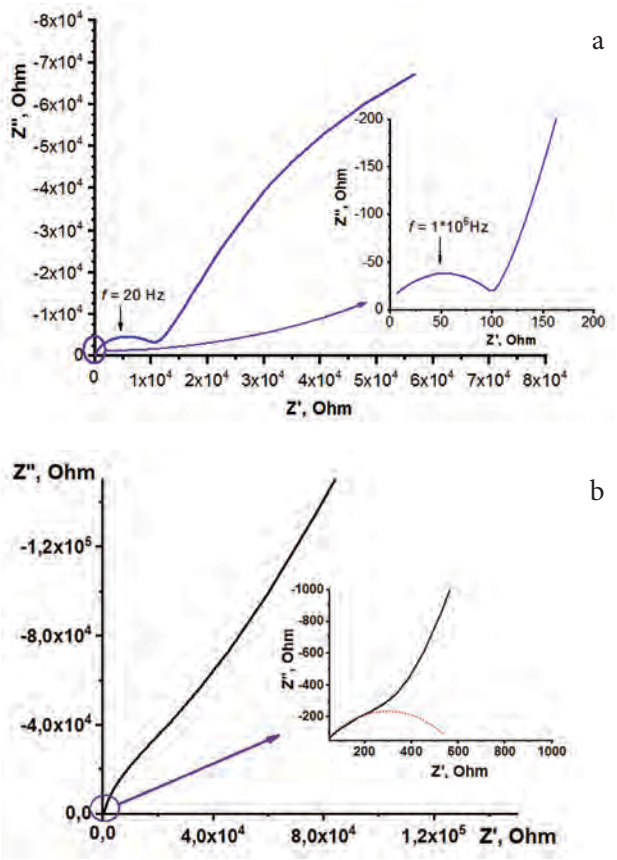

Fig. 4. Complex impedance diagram of $La_{0.67}Li_{0.2}Ti_{0.8}Al_{0.2}O_3$ (a) and $La_{0.5}Li_{0.5}TiO_3$ (b) at room temperature.

The results of the frequency investigation of $La_{0.67}Li_xTi_{1-x}Al_xO_3$ ceramics can be analyzed as four types of dependencies: complex impedance (Z*), complex admittance (Y*), complex permittivity (ε*), and complex electric modulus (M*) [20–22]. These complex quantities are interrelated: $M^* = 1/\varepsilon^* = j\omega CoZ^* = j\omega Co(1/Y^*)$, where ω is the angular frequency and Co is the capacitance of empty cell (where j = -1). Initially, the results of the frequency investigation of PTCR materials were obtained as Z" = *f*(Z') relations (**Fig. 4a**). There are three semicircles on the complex impedance diagram at room temperature for $La_{0.67}Li_{0.2}Ti_{0.8}Al_{0.2}O_3$ solid solution.

For comparison, we present impedance diagrams of $La_{0.5}Li_{0.5}TiO_3$. **Fig. 4b** shows the complex impedance diagram at room temperature for the $La_{0.5}Li_{0.5}TiO_3$. One semicircle depressed below the real axis, part of a second semicircle, and a spike at the lowest frequencies are observed. The arc at the highest frequencies is presented in the inset of **Fig. 4b**.

The appearance of three semicircles in the Cole-Cole plots indicates that there are three relaxation mechanisms, which may be due to grain, grain boundary, and electrode polarization. Generally, the arc at high frequency refers to bulk, at low frequency refers to electrode polarization, and middle-frequency area - to grain boundary. The good separation of these semicircles in $La_{0.67}Li_xTi_{1-x}Al_xO_3$ is ascribed to the small pore size. If the pore size is greater than 1 μm, it would lead to the overlapping of the semicircles like in $La_{0.5}Li_{0.5}TiO_3$ [8].

The dielectric constant was calculated from an impedance measurement. **Fig. 5** shows dielectric constant (Fig. 5a) and dielectric loss (Fig. 5b) versus frequency at room temperature. All $La_{0.67}Li_xTi_{1-x}Al_xO_3$ samples have a high dielectric constant value $\varepsilon' > 10^5$ at low frequencies ($f \leq 10$ Hz). These values are close for ones of the samples of the orthorhombic high-temperature phases $La_{0.67}Li_{0.2}Ti_{0.8}Al_{0.2}O_3$ and $La_{0.67}Li_{0.25}Ti_{0.75}Al_{0.25}O_3$ [9, 10]. Whereas it has been shown that $La_{0.5}Li_{0.5}TiO_3$ sample has a high $\varepsilon' > 10^4$ at low frequencies ($f \leq 10$ Hz).

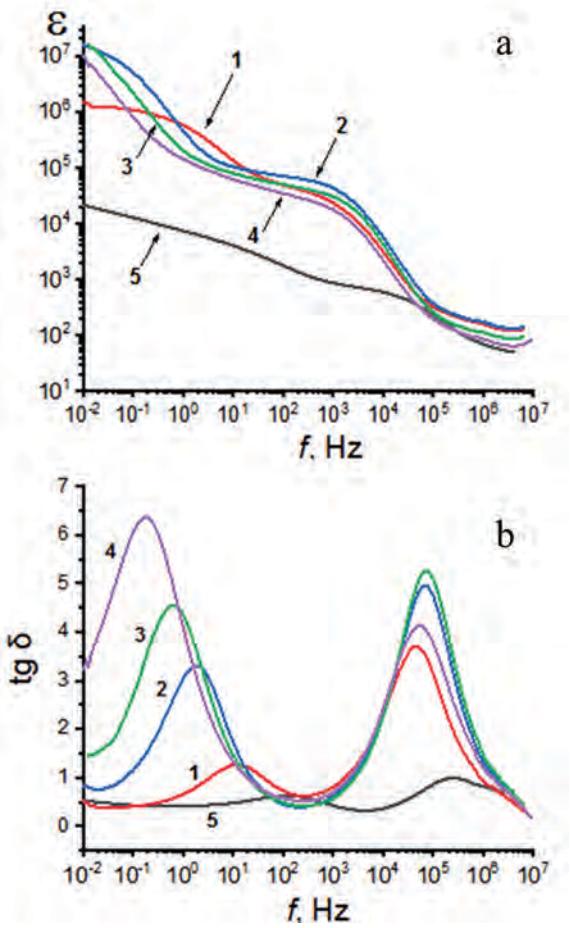

Fig. 5. Dielectric constant (a) and dielectric loss tangent (b) of $La_{0.67}Li_xTi_{1-x}Al_xO_3$ at x = 0.15 (1), 0.20 (2), 0.25 (3), 0.3 (4) and $La_{0.5}Li_{0.5}TiO_3$ (5).

Transport of Li ions in $La_{0.5}Li_{0.5}TiO_3$ occurs via vacancies in the A-site of the perovskite ABO_3 structure. Lithium ions are believed to move transport through the so-called structural conduction channels, i.e. "bottlenecks" formed by oxygen ions. Li ions are located at the center of the square planar windows connecting contiguous oxygen sites (**Fig. 6**). [14]. The high value of the dielectric constant for the $La_{0.67}Li_xTi_{1-x}Al_xO_3$ is attributed to the motion of charge carriers (Li ions) both inside and between unit cells. It should be noted that lithium ion's movement can contribute to both ionic conductivity and polarization. When lithium ions move from one electrode to another, such motion contributes to ionic conductivity. At the same time, if the motion of lithium ions in structural channels is limited, for example by lanthanum ions, then such displacements of lithium ions contribute to polarization.

In complex perovskites, the A-sites are shared by ions of very different sizes such as La^{3+} and Li^+ and vacancies whereas the B-sites are also shared by ions of different charges and sizes (**Fig. 6**).

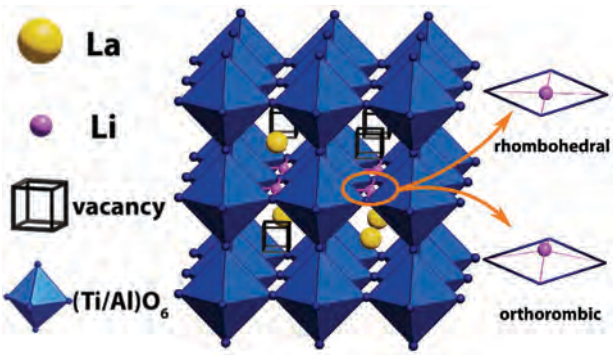

Fig. 6. Schematic representation of the difference in the rhombohedral and orthorhombic $La_{0.67}Li_xTi_{1x}Al_xO_3$ structure.

La ions occupy A sites, while Li ions are located at the A-cage faces of the perovskite. The Li^+ ions present a distorted square planar coordination and are located in interstitial positions of the structure, which could explain the very high ionic conductivity of this type of material [11]. The very high dielectric constant of this type of material seems to be related to the location of the lithium atoms within the interstitial positions, providing a great number of sites for the atoms to move through. Compared with the $La_{0.5}Li_{0.5}TiO_3$, compositions of the $La_{0.67}Li_{x-}$

$Ti_{1-x}Al_xO_3$ system have a lower number of Li^+ and a bigger number of structural vacancies. These conditions cause a lower possibility for Li^+ - V_{Li^+} interactions and enhanced opportunities for Li^+ movement. That is why materials synthesized have a higher dielectric constant than the conventional $La_{0.5}Li_{0.5}TiO_3$.

It should be noted that the dielectric constant and dielectric loss tangent slightly depends on the content of lithium and aluminum in $La_{0.67}Li_xTi_{1-x}Al_xO_3$ system.

CONCLUSIONS. It has been shown that single-phase solid solutions $La_{0.67}Li_xTi_{1-x}Al_xO_3$ ($0.15 \le x \le 0.3$) synthesized by solid-state reaction technique are formed at temperatures higher than 1200 °C. The dielectric properties of ceramic materials have been studied by impedance spectroscopy. Using light optical microscopy shown that the grain size of ceramics in $La_{0.67}Li_xTi_{1-x}Al_xO_3$ system slightly increases from 6.1 μm (x=0.15) to 7.7 μm (x=0.3). Materials exhibit high dielectric constant values ($\varepsilon \sim 4 \cdot 10^5$ at 1 Hz) in all ceramic samples that can be explained by the high ionic conductivity of this material. The materials synthesized in $La_{0.67}Li_xTi_{1-x}Al_xO_3$ system have a higher dielectric constant than the conventional $La_{0.5}Li_{0.5}TiO_3$. The dielectric losses increase with increasing lithium concentration that can be attributed to the fact that the size of the structural domains decreases with increasing the annealing temperature.

ACKNOWLEDGEMENTS. The work was supported by the Research program of the Ukrainian National Academy of Sciences "New functional substances and materials for chemical production" (Fine Chemicals), project № 0119U101351.

СИНТЕЗ ТА ДІЕЛЕКТРИЧНІ ВЛАСТИВОСТІ КЕРАМІКИ $La_{0,67}Li_xTi_{1-x}Al_xO_3$

Т. О. Плутенко, О. І. В'юнов *, Б. С. Хоменко, А. Г. Білоус

Інститут загальної та неорганічної хімії ім. В. І. Вернадського
** e-mail: vyunov@ionc.kiev.ua*

Показано, що однофазні тверді розчини в системі $La_{0,67}Li_xTi_{1-x}Al_xO_3$ в концентраційному інтервалі $0{,}15 \le x \le 0{,}3$, синтезовані методом твердофазних реакцій, утворюються за температур вище 1200 °С. Тверді розчини $La_{0,67}Li_xTi_{1-x}Al_xO_3$ (де $0{,}15 \le x \le 0{,}3$) мають ромбоедричну структуру перовскіту. Параметри елементарної комірки залежать від концентрації Li/Al.

Із ростом концентрації x об'єм елементарної комірки лінійно зменшується через різницю в іонних радіусах алюмінію та титану. Ця залежність підпорядковується закону Вегарда, що вказує на утворення неперервного ряду твердих розчинів $La_{0,67}Li_xTi_{1-x}Al_xO_3$ (де $0{,}15 \le x \le 0{,}3$).

Методом оптичної спектроскопії було показано, що розмір зерен кераміки $La_{0,67}Li_xTi_{1-x}Al_xO_3$ незначно зростає зі збільшенням концентрації літію/алюмінію. Цей факт можна пояснити підвищенням температури спікання зі збільшенням. Зі зростанням температури спікання в $La_{0,67}Li_xTi_{1-x}Al_xO_3$ збільшується розмір зерен, що супроводжується зменшенням кількості зерен, отже, загальна площа границь зерен зменшується. Дослідження за допомогою методу комплексного імпедансу продемонстрували три півкола на діаграмі Коул –

Коула, які можна віднести до електрично неоднорідних за властивостями ділянок зерен кераміки. Поява трьох напівкіл на діаграмах Коул – Коула вказує на те, що існує три механізми релаксації. Напівколо за високої частоти належить до об'ємної частини зерна, на низькій частоті – до поляризації електродів, а область середньої частоти – до властивостей границі зерен. Діелектричну проникність розраховували за даними вимірювань комплексного імпедансу. Показано, що зразки системи $La_{0,67}Li_xTi_{1-x}Al_xO_3$ мають велике значення діелектричної проникності $\varepsilon' > 10^5$ на низьких частотах ($f \leq 10$ Hz). Водночас зразок $La_{0,5}Li_{0,5}TiO_3$ має високий значення діелектричної проникності $\varepsilon' > 10^4$ на низьких частотах ($f \leq 10$ Гц), що можна пояснити високою іонною провідністю цього матеріалу. Синтезовані матеріали, леговані алюмінієм $La_{0,67}Li_xTi_{1-x}Al_xO_3$, мають вищу діелектричну проникність, ніж $La_{0,5}Li_{0,5}TiO_3$. Діелектричні втрати зростають зі збільшенням концентрації літію у $La_{0,67}Li_xTi_{1-x}Al_xO_3$, що можна пояснити зменшенням розмірів структурних доменів зі збільшенням температури відпалу.

Ключові слова: твердий розчин, титанат-алюмінат літію-лантану, комплексний імпеданс, діелектричні властивості.

ЛИТЕРАТУРА

1. Оксидные литийпроводящие твердые электролиты. / Белоус А. Г., Кобилянская С. Д. - К.: Наукова думка, 2018. - 319 с. ISBN: 978-966-00-1614-9.
2. Belous A. G. Synthesis and electrophysical properties of novel lithium ion conducting oxides // Solid State Ionics. - 1996. - V. 90, № 1–4. – P. 193–196. https://doi.org/10.1016/S0167-2738(96)00406-7.
3. Белоус А. Г., Бутко В. И., Новицкая Г. Н., Полянецкая С. В., Поплавко Ю. М., Хоменко Б. С. Электропроводность перовскитов $La_{2/3-x}M_{3x}TiO_3$ // Украинский физический журнал. – 1986. – Т. 31. – С. 576–581. https://doi.org/10.5281/zenodo.4091576.
4. Белоус А. Г., Новицкая Г. Н., Полянецкая С. В., Горников Ю. И. Исследование сложных оксидов состава $La_{2/3-x}Li_{3x}TiO_3$ // Изв. АН СССР. Неорган. материалы. – 1987. – Т. 23, № 3. – С. 470. https://doi.org/10.5281/zenodo.4074927.
5. Stramare S., Thangadurai V., Weppner W. Lithium lanthanum titanates: a review // Chemistry of materials. – 2003. – V. 15, № 21. - P. 3974–3990. https://doi.org/10.1021/cm0300516.
6. Mehrer H. Fast ion conductors // Diffusion in Solids: Fundamentals, Methods, Materials, Diffusion-Controlled Processes, 2007. – P. 475–490. ISBN: 3540714863. https:// doi.org/10.1007/978-3-540-71488-0_27.
7. Morata-Orrantia A., García-Martín S., Morán E., Alario-Franco M. Á. A New $La_{2/3}Li_xTi_{1-x}Al_xO_3$ Solid Solution: Structure, Microstructure, and Li^+ Conductivity // Chemistry of materials. - 2002. - V. 14, № 7. – P. 2871–2875. https://doi.org/10.1021/cm011149s.

8. Morata-Orrantia A., García-Martín S., Alario-Franco M. A. Optimization of lithium conductivity in La/Li titanates // Chemistry of materials. – 2003. – V. 15, № 21. – P. 3991–3995. https://doi.org/10.1021/cm0300563.
9. García-Martín S., Morata-Orrantia A., Aguirre M. H., Alario-Franco M. Á. Giant barrier layer capacitance effects in the lithium ion conducting material $La_{0.67}Li_{0.25}Ti_{0.75}Al_{0.25}O_3$ // Applied Physics Letters. – 2005. – V. 86, № 6. – P. 043110. https://doi.org/10.1063/1.1852717.
10. García-Martín S., Morata-Orrantia A., Alario-Franco M. Á. Influence of the crystal microstructure on the dielectric response of the $La_{0.67}Li_{0.2}Ti_{0.8}Al_{0.2}O_3$ // Journal of applied physics. – 2006. – V. 100, № 7. – P. 054101. https://doi.org/10.1063/1.2221528.
11. Rivera A., León C., Santamaría J., Várez A., V'yunov O., Belous A., Alonso J., Sanz J. Percolation-Limited Ionic Diffusion in $Li_{0.5-x}Na_xLa_{0.5}TiO_3$ Perovskites ($0 \le x \le 0.5$) // Chemistry of materials. – 2002. – V. 14, № 12. – P. 5148–5152. https://doi.org/10.1021/CM0204627.
12. Amador U., García-Martín S., Morata-Orrantia A., Rodríguez-Carvajal J., Alario-Franco M. Á. Structure and Microstructure Study of Oxides of the $La_{2/3x}Li_{3x}TiO_3$-family // MRS Online Proceedings Library Archive. – 2008. – V. 1126. – P. S14–06.
13. García-Martín S., Morata-Orrantía A., Alario-Franco M., Rodríguez-Carvajal J., Amador U. Beyond the structure-property relationship paradigm: influence of the crystal structure and microstructure on the Li^+ conductivity of $La_{2/3}Li_xTi_{1x}Al_xO_3$ oxides // Chemistry. A European Journal. – 2007. – V. 13, № 19. – P. 5607. https://doi.org/10.1002/chem.200700235.
14. Alonso J. A., Sanz J., Santamaría J., León C., Várez A., Fernández-Díaz M. T. On the location of Li^+ cations in the fast Li-cation conductor $La_{0.5}Li_{0.5}TiO_3$ perovskite // Angewandte Chemie. – 2000. – V. 112, № 3. – P. 633–635. https://doi.org/10.1002/(SICI)1521-3773(20000204)39:3<619::AID-ANIE619>3.0.CO;2-O.
15. Le Bail A. Whole powder pattern decomposition methods and applications: A retrospection // Powder Diffraction. – 2005. – V. 20, № 4. – P. 316–326. https://doi.org/10.1154/1.2135315.
16. Collins T. J. High-content screening // BioTechniques. – 2007. – V. 43, № 1. – P. 25–29. https://doi.org/10.2144/000112517.
17. ISO 13383-1:2016 Fine ceramics (advanced ceramics, advanced technical ceramics) - Microstructural characterization - Part 1: Determination of grain size and size distribution (ISO 13383-1:2012). – Geneva, Switzerland: International Organization for Standardization, 2016. – 29 p.
18. Yokoyama M., Ota T., Yamai I., Takahashi J. Flux growth of perovskite-type $La_{2/3}TiO_{3-x}$ crystals // Journal of crystal growth. – 1989. – V. 96, № 3. – P. 490–496. https://doi.org/10.1016/0022-0248(89)90043-2.
19. Rahaman M. N. Ceramic processing // Kirk-Othmer Encyclopedia of Chemical Technology. – 2014. – P. 1–98. https://doi.org/10.1002/0471238961.03051801052319 21.a01.pub2.
20. Morrison F. D., Sinclair D. C., West A. R. Characterization of lanthanum-doped barium titanate ceramics using impedance spectroscopy // Journal of the American Ceramic Society. – 2001. – V. 84, № 3. –

P. 531–538. https://doi.org/10.1111/j.1151-2916.2001.tb00694.x.
21. Morrison F. D., Sinclair D. C., West A. R. An Alternative Explanation for the Origin of the Resistivity Anomaly in La-Doped $BaTiO_3$ // Journal of the American Ceramic Society. – 2001. – V. 84, № 2. – P. 474–76. https://doi.org/10.1111/j.1151-2916.2001.tb00684.x.
22. Abram E. J., Sinclair D. C., West A. R. A strategy for analysis and modelling of impedance spectroscopy data of electroceramics: doped lanthanum gallate // Journal of Electroceramics. – 2003. – V. 10, № 3. – P. 165–177. https://doi.org/10.1023/B:JECR.0000011215.56084.87.
23. Gangadharudu D., Babu Y. N. C. R., Rao B. V., Rao K. S. Dielectric Spectroscopy Studies on Lead Sodium Bismuth Potasium Neobate (PNBKN) Ceramic // International Journal of Advanced Research in Physical Science. – 2015. – V. 2, № 3. – P. 7–21.

REFERENCES

1. Belous, A. G.; Kobylianska, S. D., *Lithium conducting solid oxide electrolytes*. Naukova Dumka: Kyiv, 2018; p 318. [in Russian]. ISBN: 978-966-00-1614-9.
2. Belous, A. G., Synthesis and electrophysical properties of novel lithium ion conducting oxides. *Solid State Ionics* **1996,** *90* (1-4), 193–196. https://doi.org/10.1016/S0167-2738(96)00406-7.
3. Belous, A. G.; Butko, V. I.; Novitskaya, G. N.; Polyanetskaya, S. V.; Poplavko, Y. M.; Khomenko, B. S., Electrical conductivity of the perovskites $La_{2/3-x}M_{3x}TiO_3$. *Ukrainian Journal of Physics* **1986,** *31*, 576-581. [in Russian].
4. Belous, A. G.; Novitskaya, G. N.; Polyanetskaya, S. V.; Gornikov, Y. I., Investigation into complex oxides of $La_{2/3-x}Li_{3x}TiO_3$ composition. *Izv. Akad. Nauk SSSR, Neorg. Mater* **1987,** *23* (3), 470-472. [in Russian]. https://doi.org/10.5281/zenodo.4074927.
5. Stramare, S.; Thangadurai, V.; Weppner, W., Lithium lanthanum titanates: a review. *Chem. Mater.* **2003,** *15* (21), 3974-3990. https://doi.org/10.1021/cm0300516.
6. Mehrer, H., Fast ion conductors. In *Diffusion in Solids: Fundamentals, Methods, Materials, Diffusion-Controlled Processes*, 2007; pp 475-490. ISBN: 3540714863. https://doi.org/10.1007/978-3-540-71488-0_27.
7. Morata-Orrantia, A.; García-Martín, S.; Morán, E.; Alario-Franco, M. Á., A New $La_{2/3}Li_xTi_{1-x}Al_xO_3$ Solid Solution: Structure, Microstructure, and Li^+ Conductivity. *Chem. Mater.* **2002,** *14* (7), 2871-2875. https://doi.org/10.1021/cm011149s.
8. Morata-Orrantia, A.; García-Martín, S.; Alario-Franco, M. A., Optimization of lithium conductivity in La/Li titanates. *Chem. Mater.* **2003,** *15* (21), 3991-3995. https://doi.org/10.1021/cm0300563.
9. García-Martín, S.; Morata-Orrantia, A.; Aguirre, M. H.; Alario-Franco, M. Á., Giant barrier layer capacitance effects in the lithium ion conducting material $La_{0.67}Li_{0.25}Ti_{0.75}Al_{0.25}O_3$. *Appl. Phys. Lett.* **2005,** *86* (6), 043110. https://doi.org/10.1063/1.1852717.
10. García-Martín, S.; Morata-Orrantia, A.; Alario-Franco, M. Á., Influence of the crystal microstructure on the dielectric response of the $La_{0.67}Li_{0.2}Ti_{0.8}Al_{0.2}O_3$. *J. Appl. Phys.* **2006,** *100* (7), 054101. https://doi.org/10.1063/1.2221528.
11. Rivera, A.; León, C.; Santamaría, J.; Várez, A.; V'yunov, O.; Belous, A.; Alonso, J.;

Sanz, J., Percolation-Limited Ionic Diffusion in $Li_{0.5-x}Na_xLa_{0.5}TiO_3$ Perovskites ($0 \leq x \leq 0.5$). *Chem. Mater.* **2002,** *14* (12), 5148-5152. https://doi.org/10.1021/CM0204627.
12. Amador, U.; García-Martín, S.; Morata-Orrantia, A.; Rodríguez-Carvajal, J.; Alario-Franco, M. Á., Structure and Microstructure Study of Oxides of the $La_{2/3-x}Li_{3x}TiO_3$-family. *MRS Online Proceedings Library Archive* **2008,** *1126*, S14-06.
13. García-Martín, S.; Morata-Orrantía, A.; Alario-Franco, M.; Rodríguez-Carvajal, J.; Amador, U., Beyond the structure-property relationship paradigm: influence of the crystal structure and microstructure on the Li^+ conductivity of $La_{2/3}Li_xTi_{1-x}Al_xO_3$ oxides. *Chemistry. A European Journal* **2007,** *13* (19), 5607. https://doi.org/10.1002/chem.200700235.
14. Alonso, J. A.; Sanz, J.; Santamaría, J.; León, C.; Várez, A.; Fernández-Díaz, M. T., On the location of Li^+ cations in the fast Li-cation conductor $La_{0.5}Li_{0.5}TiO_3$ perovskite. *Angew. Chem.* **2000,** *112* (3), 633-635. https://doi.org/10.1002/(SICI)1521-3773(20000204)39:3<619::AID-ANIE619>3.0.CO;2-O.
15. Le Bail, A., Whole powder pattern decomposition methods and applications: A retrospection. *Powder Diffr.* **2005**, *20* (4), 316-326. https://doi.org/10.1154/1.2135315.
16. Collins, T. J., High-content screening. *BioTechniques* **2007,** *43* (1), 25-29. https://doi.org/10.2144/000112517.
17. AENOR, ISO 13383-1:2016 Fine ceramics (advanced ceramics, advanced technical ceramics) - Microstructural characterization - Part 1: Determination of grain size and size distribution (ISO 13383-1:2012). International Organization for Standardization: Geneva, Switzerland, 2016; p 29.
18. Yokoyama, M.; Ota, T.; Yamai, I.; Takahashi, J., Flux growth of perovskite-type $La_{2/3}TiO_{3-x}$ crystals. *J. Cryst. Growth* **1989,** *96* (3), 490-496. https://doi.org/10.1016/0022-0248(89)90043-2.
19. Rahaman, M. N., Ceramic processing. *Kirk-Othmer Encyclopedia of Chemical Technology* **2000**, 1-98. https://doi.org/10.1002/0471238961.0305180105231921.a01.pub2.
20. Morrison, F. D.; Sinclair, D. C.; West, A. R., Characterization of lanthanum-doped barium titanate ceramics using impedance spectroscopy. *J. Amer. Ceram. Soc.* **2001,** *84* (3), 531-538. https://doi.org/10.1111/j.1151-2916.2001.tb00694.x.
21. Morrison, F. D.; Sinclair, D. C.; West, A. R., An Alternative Explanation for the Origin of the Resistivity Anomaly in La-Doped $BaTiO_3$. *J. Amer. Ceram. Soc.* **2001,** *84* (2), 474-76. https://doi.org/10.1111/j.1151-2916.2001.tb00684.x.
22. Abram, E. J.; Sinclair, D. C.; West, A. R., A strategy for analysis and modelling of impedance spectroscopy data of electroceramics: doped lanthanum gallate. *J. Electroceram.* **2003,** *10* (3), 165-177. https://doi.org/10.1023/B:JECR.0000011215.56084.87.
23. Gangadharudu, D.; Babu, Y. N. C. R.; Rao, B. V.; Rao, K. S., Dielectric Spectroscopy Studies on Lead Sodium Bismuth Potasium Neobate (PNBKN) Ceramic. *International Journal of Advanced Research in Physical Science* **2015,** *2* (3), 7-21.

Стаття надійшла 28.10.2020